International Journal of Automotive Technology, Vol. 6, No. 3, pp. 259–268 (2005)

1229–9138/2005/021–09

PLASTIC STRAIN RATIOS AND PLANAR ANIOSOTROPY OF AA5182/POLYPROPYLENE/AA5182 SANDWICH SHEETS

K. J. KIM*

CAE Team, Ssang Yong Motor Company, 150-3 Chilgoi-dong, Pyungtaek-si, Gyeonggi 459-711, Korea

(Received 3 November 2004; Revised 8 October 2004)

ABSTRACT–In order to analyze the sheet drawability, the measurement of the plastic strain ratio was carried out for the 5182 aluminum alloy sheets in which were cold rolled without lubricaton and subsequent recrystallization annealing. The average plastic strain ratio of the 5182 aluminum sheets was 1.50. It was considered that the higher plastic strain ratio was resulted from the ND//<111> component evolved during rolling and maintained during annealing. The AA5182/ polypropylene/AA5182 (AA/PP/AA) sandwich sheets of the 5182 aluminum alloy skin sheet and the polypropylene core sheet with high formability have been developed for application for automotive body panels in future light weight vehicles with significant weight reduction. The AA/PP/AA sandwich sheets were fabricated by the adhesion of the core sheet and the upper and lower skin sheets. The AA/PP/AA sandwich sheet had high plastic strain ratio (1.58), however, the planar anisotropy of the sandwich sheet was little changed after fabrication. The optimum combination of directionality of the upper and lower skin sheets having high plastic strain ratio and low planar anisotropy was calculated theoretically and an advanced process for producing the sandwich sheets with high plastic strain ratio was proposed. The developed sandwich sheets have a high average plastic strain ratio of 1.55 and a low planar anisotropy of 0.17, which was improved more by 3.2 times than that of 5182 aluminum single sheet.

KEY WORDS : Sandwich sheet, AA5182 skin, Texture, Plastic strain ratio, Drawability and planar anisotropy

1. INTRODUCTION

In recent years, the effort to decrease environmental pollution and improve the fuel efficiencies has been made continuously in the automobile industry, and the legal sanction against air pollution is getting tightened. As part of this effort, lightweight vehicles have become the center of attention, and the effort to replace from a steel sheet to a lighter material for automotive body panels has been made. In addition, various metal-plastic laminates and sandwich sheets have been developed in order to reduce the vehicle weight for some high performance automobiles. The AA5182/ polypropylene/AA5182 (AA/ PP/AA) sandwich sheet consists of two 5182 aluminum skins with a thermoplastic polypropylene core in between in order to achieve the lightest weight per unit area when flexural rigidity is the design criterion. Since the sandwich sheet is made by roll bonding polypropylene with low density for a core and aluminum skins sheet with relatively high strength together, it has great potential materials in applying to automotive body panels due to its lightweight (Veenstra, 1993; Shin *et al.*, 1999; Rhee *et al.*, 2000; Kim *et al.*, 2003). One of the important characteristics for the automotive outer sheet is the excellent formability. According to the sandwich sheet used in this study, because the elongation of the polypropylene core sheet is over 500%, it is expected to contribute to the formability improvement of the sandwich sheet, though the formability of 5182 aluminum skin sheets is considerably lower than the steel sheets. As the result, the drawability of the sandwich sheets could be lower than the existing steel sheets. In order to apply the sandwich sheets to the automotive body panels, the texture evolution caused by rolling and the control against planar anisotropy on the 5182 aluminum skin sheets is needed in order to improve the plastic strain ratio (R-value or drawability) of the aluminum alloys fabricated by the rolling process. In addition, the complete bonding technique between the polypropylene core sheet and the 5182 aluminum skin sheet should be also needed.

The drawability of roll formed metal sheets is closely related with textures (Lee and Oh, 1985; Lequeu and Jonas, 1988; Hutchinson, 1989; Kamijo *et al.*, 1992; 1993; Hu *et al.*, 1996; Hasegawa *et al.*, 1998; Park, 1999; Saito, 2000; Pithan *et al.*, 2000). For increasing the plastic strain ratio in the aluminum alloy sheets, which are FCC metals, the sheets should be fabricated that they

*Corresponding author. e-mail: kjkimfem@smotor.com

have well evolved shear texture components. When the sheets were loaded higher by shear deformation, the friction coefficient, μ was increased. Among shear deformation texture, if, especially, γ-fiber ND//<111> (Hutchinson, 1989; Kamijo *et al.*, 1993; Saito *et al.*, 2000; Pithan *et al.*, 2000) was well evolved, the planar anisotropy decreased and the deep drawing capability increased, on the other hand, if rot-CND {100}<110> component was well evolved, the planar anisotropy increased (Lee and Oh, 1985; Lequeu and Jonas, 1988; Saito *et al.*, 2000; Asbeck and Mecking, 1978; Truszkowski *et al.*, 1980; Truszkowski *et al.*, 1982; Major, 1992; Holscher *et al.*, 1994; Choi and Lee, 1995; Choi *et al.*, 1997; Kamijo *et al.*, 1972; Kamijo and Fukutomi, 1995; Kim, 1999; Lee *et al.*, 1997; Lee and Duggan, 1991; Lee *et al.*, 1994).

T. Kamijo *et al.* (Kamijo *et al.*, 1972; Kamojo and Fakutoni, 1995) had fabricated the aluminum alloy sheets which had a higher R-value by using warm rolling, however, the main component of shear textures was rot-C_{ND} {100}<110> and the planar anisotropy of these sheets was too higher and then the average R-value of these sheets was lowered. As above, processes for maximizing the shear texture evolution were extremely limited. Special ones (ECAP; equal channel angular process, warm rolling, asymmetric rolling, etc), when the shear deformation was maximized, the *earing* occurred highly because of high planar anisotropy (Kamijo *et al.*, 1972; Kamijo and Fukutomi, 1995; Kim, 1999; Lee *et al.*, 1997; Lee and Duggan, 1991). The main purpose was to fabricate the sheets having lower planar anisotropy and higher drawability for applying the sandwich sheets for automotive body panels in the present study. Since the anisotropy and the drawability were highly dependent on the R-value, the R-value test and calculation were carried out for drawability evaluation of the 5182 aluminum skins and the sandwich sheets. For improving the anisotropy of the sandwich sheets, the directionality combination of the upper and lower aluminum skins was theoretically calculated. Through this calculation, a fabrication process for the sandwich sheet was proposed. Moreover, the drawability evaluation of the 5182 aluminum skins and the sandwich sheets brought about a fundamental improvement based on theoretical and experimental analysis of the multi-layered sheets which had the strong planar anisotropy.

2. EXPERIMENTAL PROCEDURE

2.1. Roll Forming and Annealing of AA5182 Skin Sheets

5182 aluminum alloys of 4.5 mm in initial thickness was fabricated by hot rolling in Daehan Wire Co. and the homogenization treatment at 500°C was carried out for cold rolling. The cold rolling conditions of the 5182 aluminum alloys were roll diameter (127 mm), rolling temperature (room temperature), rolling speed (400 rpm), total by three pass cold rolled, total reduction ratio (92.8%; over 50% reduction per 1 pass) and the *l/d* parameters (6.77) (Kamijo *et al.*, 1992; Kamijo *et al.*, 1993; Hu *et al.*, 1996; Hasegawa *et al.*, 1998; Park, 1999; Saito *et al.*, 2000; Pithan *et al.*, 2000; Asbeck and Mecking, 1989; Truszkowski *et al.*, 1980, 1982), and various sheets having shear textures were obtained. For applying the high friction between the roll bite and the specimen, the lubrication was not applied to the roll bite in order to achieve more evolved shear deformation textures. The formation of recrystallization texture was investigated from the heat treatment of the specimens, which were well evolved on the shear texture from rolling. In order to examine the recrystallization texture of the 5182 aluminum sheets, annealing was conducted on a salt bath with various holding time (0 sec, 60 sec, 180 sec, 1,200 sec, 3,600 sec and 7,200 sec, respectively) at 350°C.

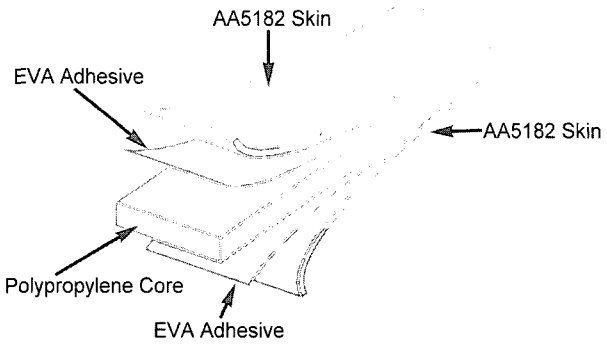

Figure 1. Schematic diagram of the AA/PP/AA sandwich sheet.

2.2. Fabrication of AA5182/Polypropylene/AA5182 Sandwich Sheets

A schematic diagram of the AA/PP/AA sandwich sheet is shown in Figure 1. The sandwich sheet was prepared by roll bonding of two 5182 aluminum skins with a pre-rolled polypropylene sheet in between at 140°C. Film type ethylene vinyl acetone (EVA) adhesives were inserted between the aluminum skin and the polypropylene core in order to achieve the appropriate bond strength. The AA/PP/AA sandwich sheets having 1.2 mm in total thickness consist of core sheet of 0.8 mm in thickness and the skin sheets of 0.2 mm in thickness were adopted for the present study.

2.3. Characterization of AA5182 and AA/PP/AA Sandwich Sheets

Specimens for the measurement of the pole figure in order to analyze the textures of the rolled aluminum sheet

were prepared after mechanical polishing and those of surface deformation layer of 10 mm in thickness were removed from chemical polishing with 10% NaOH solution in the present study. Then {111}, {200} and {220} pole figures were measured from Schultz reflection method. The measuring equipment was a Seifert 3003 and the voltage and the current were applied for 30 kV and 15 mA, respectively. Using target was the Co target, which had been well recommended in FCC metals.

The plastic strain ratio is the important barometer to evaluate deep drawing capability and the anisotropy of the sheet. In general, since the roll formed sheets have the planar anisotropy following tensile orientation, the specimens were prepared with different specimen angles, 0°, 45° and 90° to the sheet rolling direction. The plastic strain ratio (R) was measured with 2-extensometers that were installed in the tensile and transverse directions, respectively, during tensile tests (Jeong *et al.*, 1999) in order to evaluate the planar anisotropy. The plastic strain ratio is defined as shown in Equation (1). Here, ε_{22} and ε_{33} is transverse and thickness true strain, respectively.

$$R = \frac{\varepsilon_{22}}{\varepsilon_{33}} \tag{1}$$

If metals are assumed incompressible in plastic deformation, the plastic strain ratio can be changed as following Equation (2).

$$R = \frac{\varepsilon_{22}}{-(\varepsilon_{11} + \varepsilon_{22})} \tag{2}$$

Since Equation (2) is derived from the assumption that the plastic strain ratio is constant following deformation, though the plastic strain ratio is changed following tensile deformation, it is difficult to represent well. Therefore, the instantaneous plastic strain ratio (Lee and Oh, 1985; Jeong *et al.*, 1999, 2000) which was the differential value from the strain-strain values was used as described in Equation (3) in present study.

$$R_i = \frac{d\varepsilon_{22}}{d\varepsilon_{33}} \tag{3}$$

In addition, the plastic strain ratio was obtained from the average value of 0.05~0.10 tensile strain and average plastic strain ratio (R_m) and the planar anisotropy of the R-value (ΔR) were calculated from the following Eq. (4) and Equation (5), where the R_0, R_{45}, and R_{90} were the plastic strain ratio when the angles between the rolling direction and the tensile axis were 0°, 45°, and 90°, respectively.

$$R_m = \frac{R_0 + R_{90} + 2R_{45}}{4} \tag{4}$$

$$\Delta R = \frac{R_0 + R_{90} - 2R_{45}}{2} \tag{5}$$

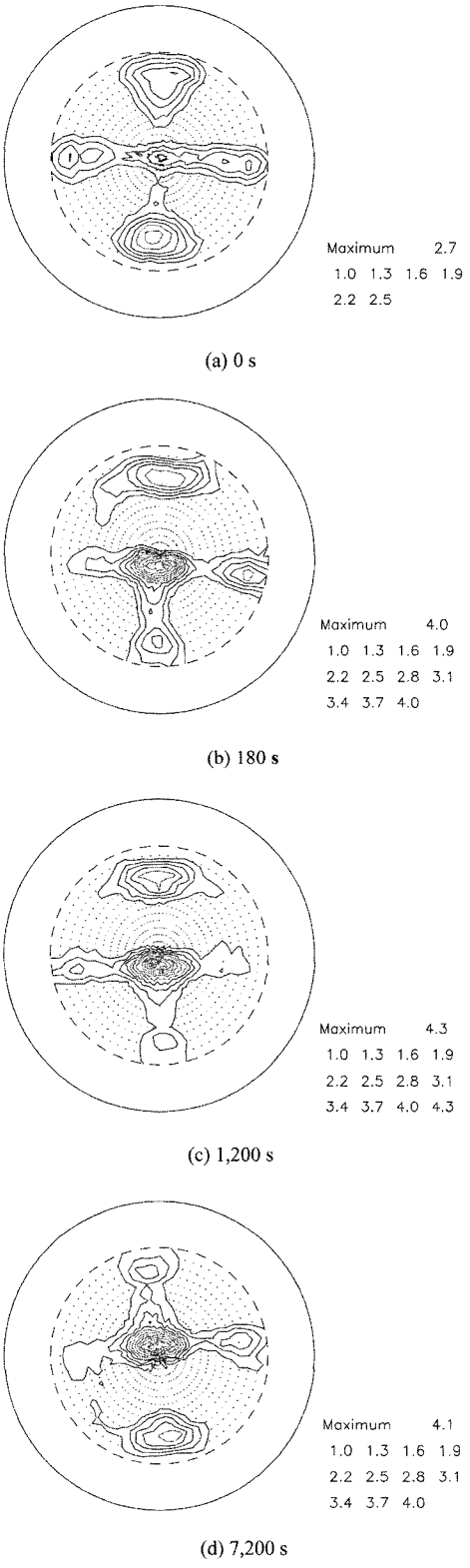

Figure 2. Measured (111) pole figures of AA5182 sheets after annealing at 350°C for (a) 0 sec, (b) 60 sec, (c) 180 sec, (d) 1,200 sec, (e) 3,600 sec and (f) 7,200 sec.

One method to evaluate the material formability is deep drawing test. Sheets that are stretched clamped at their edges are stretched by a hemispherical punch having a circular cross section for making cup shape product. The larger diameter of the sheet is, the deeper cup can be made. However, if the diameter of the sheet increased, in case of sheet having lower drawability, the successful cup couldn't be made when it reached a criterion value. Therefore, as the diameter of the sheet is different following various materials, the deep drawing capability of materials can be a characteristic material property. If the average R-value is higher, the deep drawing capability increases as well known (Jeong *et al.*, 2000; Lee, 1985). And thus, if the planar anisotropy of the R-value is higher, the *earing* (phenomenon that the edge of drawing cup have a pitch and valley shape) can easily occur and the uniform forming can't be acquired (Jeong *et al.*, 2000; Lee, 1985).

3. EXPERIMENTAL RESULTS

3.1. Rolling and Recrystallization Texture

The pole intensities of the recrystallization texture were measured after heat treatment of the sheets in which the shear deformation textures were enough developed by rolling. Figure 2 shows the change in texture developed in 5182 aluminum alloy sheet during heat treatment at 350°C with various annealing time compared to the texture before heat treatment. In case of the 5182 aluminum alloy sheet with *l/d* parameter of 6.77 (total reduction ratio of 92.8%) before heat treatment, the pole intensity of γ-fiber ND//<111> was very high. However, the pole intensity of rot-C_{ND} {001} <110> decreased but the pole intensity of γ-fiber ND//<111> increased with annealing time. In general, it is well known that the intensity of X-ray peak is lower and the broadening of the peak occurs in the material with high strain by accumulation of the dislocations, but the intensity of X-ray peak increases and the sharp peak is observed due to the rearrangement and reduction of the dislocations by recovery during heat treatment. In case of the sheet heat-treated for 60 sec in which the recovery might be occurred, γ-fiber ND//<111> didn't rotate to other orientations and the pole intensity of γ-fiber ND//<111> increased as same in case of X-ray measurement of specimens which were severely deformed then recovered. The pole intensity of rot-C_{ND} {001}<110> orientation decreased but the pole intensity of γ-fiber ND//<111> orientation increased after heat treatment for 180 sec. As shown in Figure 2(c) and (d), γ-fiber ND//<111> didn't rotate to other orientations after heat treatments for 1,200 and 7,200 sec. More detailed analysis on the

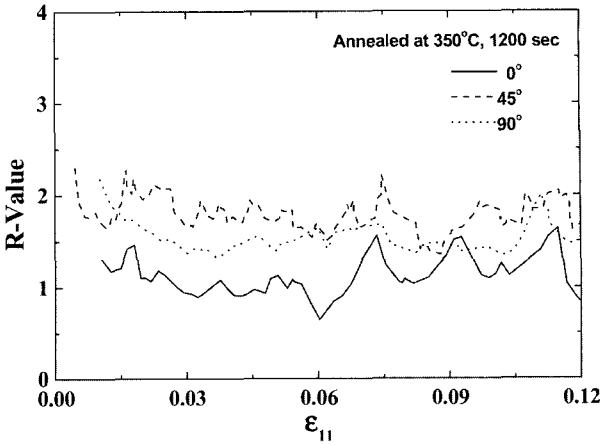

Figure 4. Measured R-values as a function of tensile strain of AA5182 sheets for different tensile orientations.

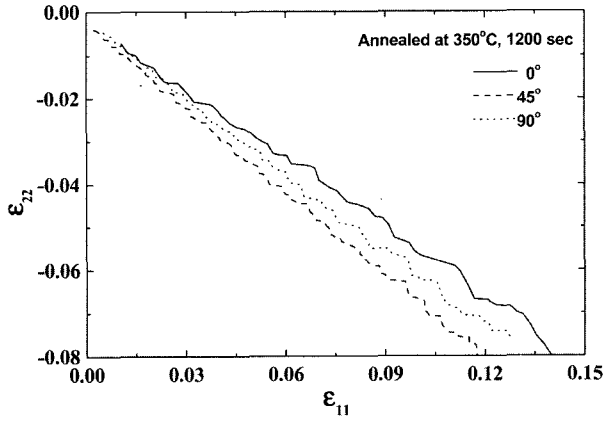

Figure 3. Measured width strain (ε_{22}) as a function of tensile strain (ε_{11}) of AA5182 sheets for different tensile orientations.

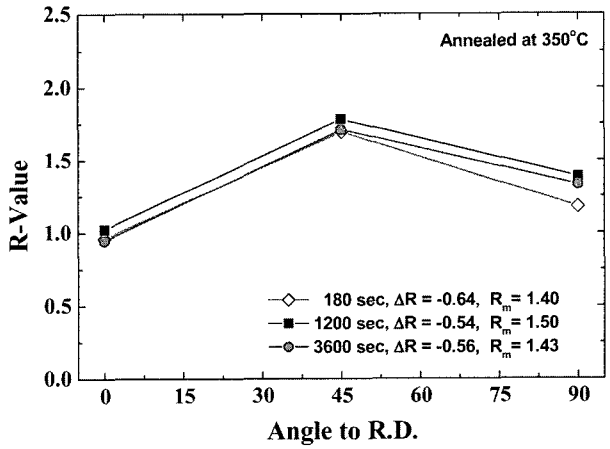

Figure 5. Measured R-values of symmetrically rolled AA5182 sheets for different annealing times.

evolution and discussion of recrystallization texture on the 5182 aluminum alloy sheet following annealing conditions is beyond the scope of the present paper and will be published elsewhere (Kim, 2005).

Figure 3 shows the measured results for the width strain vs. longitudinal (tensile direction) strain in the 5182 aluminum alloy sheets specimens which were prepared after annealing during 1,200 sec at 350°C with different specimen angles 0°, 45° and 90° to the sheet rolling direction in order to measure the planar anisotropy. It seemed that the plastic strain ratio might be the highest at the direction of 45° and the lowest at the direction of 0° because the slope at the direction of 45° was the largest and that at the direction of 0° was the smallest. Figure 4 shows the change of the plastic strain ratio of the 5182 aluminum alloy sheet following tensile deformation. As shown in Figure 4, the plastic strain ratio was the highest at the direction of 45° as predicted in the sheets. Also, the average plastic strain ratio (R_m) and the planar anisotropy (ΔR) were calculated by using the Equation (4) and (5).

Figure 5 shows the plastic strain ratio, the average plastic strain ratio and the anisotropy of the plastic strain ratio of the 5182 aluminum alloy sheets annealed with holding time for 180, 1,200 and 3,600 sec at 350°C. The plastic strain ratio was the highest with heat-treated holding time for 1,200 sec at 350°C and the average plastic strain ratio was 1.50, which was higher than those of the Al alloys reported in the literature. It resulted from that the γ-fiber ND//<111> components were developed as the preferred orientation in the sheet fabricated by the rolling process proposed in this study and didn't rotate to other orientations, and the pole intensity of γ-fiber ND// <111> components increased after recrystallization. However, the anisotropy of the plastic strain ratio was from −0.54 to −0.64, which was still high.

Table 1. Lankford values for some ideal orientations by P. Lequeu and J. J. Jonas (Lequeu and Jonas, 1998).

Ideal Orientation	R_0	R_{45}	R_{90}	R_m	$\lvert\Delta R\rvert$
{001}<110>	0.00	1.00	0.00	0.53	0.30
{111}<110>	1.84	1.89	1.95	1.91	0.04
{111}<112>	1.84	1.89	1.95	1.91	0.04
{112}<110>	0.53	1.89	1.00	1.29	0.34
{001}<100>	1.00	0.00	1.00	0.53	0.30
{110}<112>	0.50	2.09	1.00	1.35	0.46
{112}<111>	1.00	1.89	0.50	1.29	0.34
{123}<634>	0.72	1.81	0.83	1.27	0.35

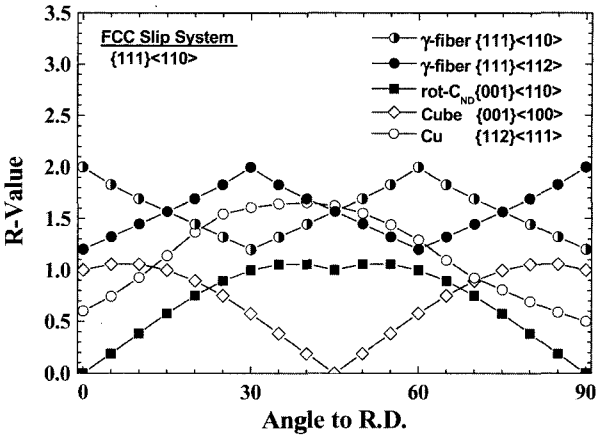

Figure 6. Calculated R-value for {111}<110>, {111} <112>, {001}<110>, {001}<100> and {112}<111> orientations.

4. DISCUSSION

4.1. Effect of Plastic Strain Ratio on Texture

Table 1 shows the plastic strain ratio of ideal orientations (about single crystals) calculated based on CMTP method by P. Lequeu and J. J. Jonas (Lequeu and Jonas, 1998). The average plastic strain ratio of γ-fiber {111}<110> and {111}<112> orientations was the highest value of 1.91 and the lowest planar anisotropy and they should generate an excellent drawability. In addition, rot-C_{ND} {001}<110> orientation, which is rotated by 45° to the ND axis of Cube {001}<100> orientation, and Cube {001}<100> orientation have the lowest plastic strain ratio and the highest anisotropy. The plastic strain ratio of the sheets having the plane strain texture with Cu {112}<111> and Br {110}<112> orientation as the preferred orientation were 1.29 and 1.35, respectively and also a little bit high as shown in Table 1. It was well known fact that the polycrystal sheets having strong γ-fiber {111}<uvw> orientation show both the highest average plastic strain ratio and the lowest planar anisotropy can be found from the empirical and calculated papers by utilizing the similar calculation method about the single crystals (Lee and Oh, 1985; Lequeu and Jonas, 1988).

In this study, the plastic stain ratio of Z {111}<110>, Y {111}<112>, Cu {112}<111>, rot-C_{ND} {001}<110> and Cube {001}<100> among several ideal orientations were calculated by Vieth-Whiteley, Fukuda, Lee methods [5,6,32], considering the slip systems and rotation of crystals as shown in Figure 6. Z {111}<110> and Y {111}<112> orientations of γ-fiber component show the highest plastic strain ratio and the Cu {112}<111> orientation is ranked to the middle one, and both rot-C_{ND} {001}<110> and Cube {001}<100> orientations show the lowest plastic strain ratio. Therefore, as the same in

the single crystal, polycrystal sheets distributed as the preferred orientation having the texture of Z {111}<110> and Y {111}<112> orientations of γ-fiber component should have the excellent drawability.

4.2. Effect of Average Plastic Strain Ratio on Sheet Drawability

There has no difference on plastic strain ratio of isotropic materials with the plane orientation. High R-value means that the resistance against thickness reduction is high during deep drawing process. In general, since the sheet material represents the planar anisotropy, the average plastic strain ratio (R_m) was calculated by using Equation (4) when the angles between the rolling direction and the tensile axis were 0°, 45° and 90°, respectively, and the average plastic strain ratio is used as a standard of the drawability. The *earing* occurred during a deep drawing process because of different R-value of each rolling direction due to the planar anisotropy. The directions, which showed higher R-value, make thin wall and ear and the directions, which showed lower R-value, make valley. This trend was well observed where the angles between the rolling direction and the tensile axis were 0°, 45° and 90°, respectively, and how to control the *earing* improvement is a important point to reduce a great loss during trimming after a deep drawing process.

Meanwhile, γ-fiber ND//<111> is the most important component to improve the sheet drawability. Especially, many interests were focused on this component through the fabrication process of the steel sheet for automobiles. Since the heterogeneous deformation (shear deformation) suppressed obviously the evolution of γ-fiber ND//<111> in BCC metals, the research groups (Sakai *et al.*, 1987; 1988; 1991) who studied primarily carried out the studies to get the plane strain texture by reducing a rolling temperature, a rolling speed and a friction coefficient. However, since FCC metals such as aluminum alloys don't commonly have γ-fiber ND//<111> in plane strain texture or recrystallization texture, the research to improve the drawability is tied-up, on the contrary, only the research to reduce the *earing* occurrence has been actively made (Kamijo *et al.*, 1979, 1995; Kim, 1999; Lee *et al.*, 1997; Lee and Duggan, 1991; Jeong *et al.*, 2000; Lee, 1985). The average plastic strain ratio of the sheets, which had γ-fiber ND//<111>, increased regardless of crystal structure such as BCC and FCC, and γ-fiber ND//<111> was also greatly affected by recrystallization behavior.

4.3. Effect of Annealing on Plastic Strain Ratio and Texture

The analysis of pole intensity of γ-fiber ND//<111> at (111) pole figure measured after annealing of the 5182 aluminum alloy sheets with holding time for 60, 180, 1,200, 3,600 and 7,200 sec at 350 was compared to the result of measured plastic strain ratio as shown in Figure 7. After annealing with holding time for 180 sec at 350°C, the pole intensity of γ-fiber ND//<111> increased rapidly and showed the maximum value at 350°C for 1,200 sec. In addition, the measured average plastic strain ratio increased proportionally with increasing the pole intensity of γ-fiber ND//<111>.

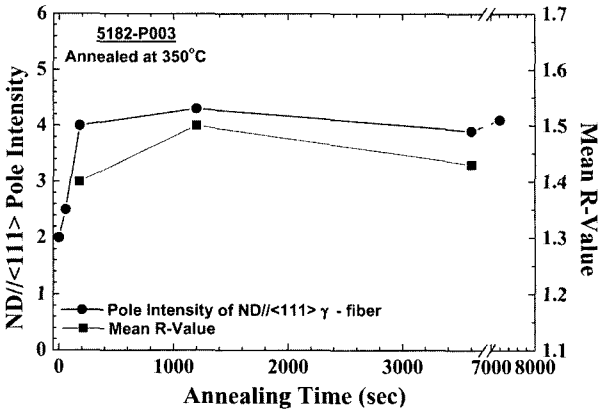

Figure 7. Measured pole intensity of ND//<111> γ-fiber and R-values of AA5182 sheets following as annealing time at 350°C.

Since the preferred orientations might rotate and change to the random orientation increasingly during annealing, the measured (111) pole figure of the 5182 aluminum alloy sheet annealed at 350°C shows that the pole intensities of rot-C_{ND} {001}<110> component have tendency to decreases with increasing annealing time as shown in Figure 2. According to previously measured reports such as the forming process by ECAP, hot rolling and asymmetric rolling, the planar anisotropy of the plastic strain ratio and the average plastic strain ratio decrease with increasing heat treatment temperature and time (Kim, 1999; Lee *et al.*, 1997; Lee and Duggan, 1991; Lee *et al.*, 1994; Baeck *et al.*, 2001; Sakai *et al.*, 2001). In present study, the planar anisotropy of the plastic strain ratio increases proportionally with the pole intensity of rot-C_{ND} {001}<110> as shown in Figure 2 and Figure 5.

4.4. Plastic Strain Ratio of Sandwich Sheet and Controls of Planar Anisotropy

The plastic strain ratio was measured on AA5182/ Polypropylene/AA5182 sandwich sheet, which consisted of the 5182 aluminum skin sheets and the polypropylene core sheet. While the average plastic strain ratio of the sandwich sheet (1.58) was higher than that the 5182 aluminum alloy single layer sheet (1.50), the planar anisotropy of plastic strain ratio was not greatly reduced depending on the high planar anisotropy of the skin sheet. Based on this result, it was tried to suggest how to

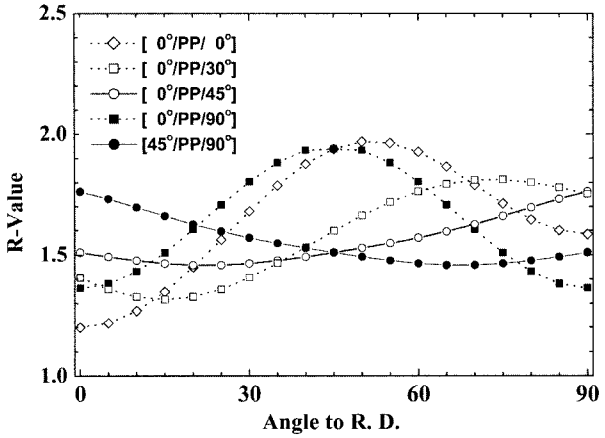

Figure 8. Calculated R-values of the AA/PP/AA sandwich sheets.

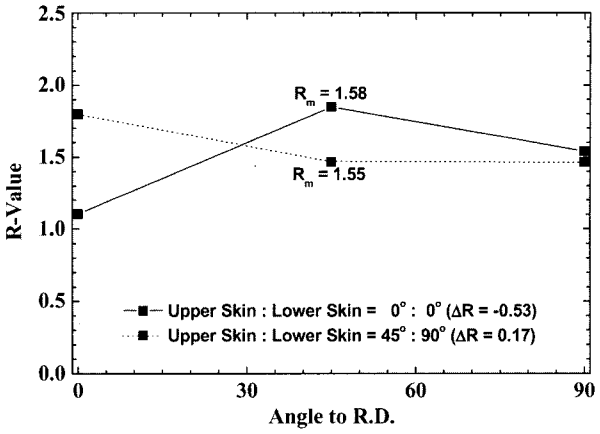

Figure 10. Measured R-values of AA/PP/AA sandwich sheets for different tensile orientation.

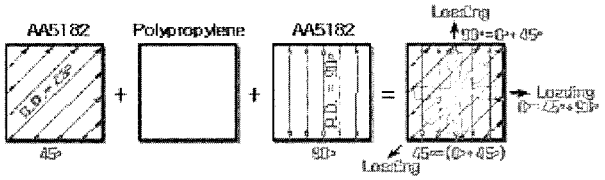

Figure 9. Idealized fabrication method to improve the planar anisotropy of the sandwich sheet.

effectively control the anisotropy of the R-value using the advantage of the sandwich sheet in present study. The control method for the planar anisotropy is shown through derivation of Equation (6) and the calculation of plastic strain ratio in sandwich sheet. The derivate process and the significance of index were shown in detail in appendix. The optimum directionality combination of the upper/lower skin sheet was calculated through the procedure in appendix in order to utilize appropriately the directionality of the sandwich sheet, which was fabricated by adhering two anisotropic 5182 aluminum skin sheets.

$$\sigma_x^{tot} = \sum_i \frac{t^i}{t^{tot}} \sigma_x^i = \sum_i \frac{t^i}{t^{tot}} \left(\frac{\bar{\sigma}^i}{\Delta \bar{\varepsilon}^i} \right) \boldsymbol{Q}^i \cdot \boldsymbol{C}^i \cdot (\boldsymbol{Q}^{-1})^i \cdot \Delta \varepsilon_x^i \quad (6)$$

Figure 8 shows the calculated results of combinations of the upper/lower skin sheets, 0°/PP/0°, 0°/PP/30°, 0°/PP/45° and 45°/PP/90°, respectively, by using the properties in Table 2 and appendix. In these results, 45°/PP/90° combination of the upper/lower skin sheets was identical with 0°/PP/45° in characteristic of the sandwich sheet. The combination that shows the highest plastic strain ratio and the lowest planar anisotropy was 45°/PP/90° combination as shown in Figure 8.

Through Figure 8, an optimum combination of the highest plastic strain ratio and the lowest planar anisotropy can be determined by utilizing the directionality, in which the upper skin of the 5182 aluminum alloy sheet was cut by 45° to the sheet rolling direction and the lower skin of that is cut by 90° to the sheet rolling direction, as shown in Figure 9. Therefore, the sandwich sheet was fabricated as a form shown in Figure 9 in order to effectively control the high anisotropy of the R-value in 5182 aluminum single layer sheet. Since the aluminum skin sheets that composed of the upper/lower skin sheet are adhered with the polypropylene core sheet, the planar anisotropy of the AA/PP/AA sandwich sheet is also high when the planar anisotropy of the skin sheet is high. The plastic strain ratio of the sandwich sheets was measured for which the angles between the rolling direction and the tensile axis case of the skin sheet were 0°, 45° and 90°, respectively. As shown in Figure 9, when the angles of the sandwich sheets between the rolling direction and the tensile axis were 0°, 45° and 90°, respectively, the upper/lower skin sheets were 45°/PP/90°, 0°/PP/45° and 0°/PP/45°, respectively, and when the specimen angle of the sandwich sheet was 45°, the angle of the upper/lower skin sheets of the sandwich sheet corresponded to 90°.

Figure 10 shows comparison of the plastic strain ratio of the AA/PP/AA sandwich sheet fabricated by an improved process (refer to Figure 9) with that of the sandwich sheet fabricated without using the directionality of the skin sheets when the angle between the tensile axis and the rolling direction of the upper/lower skin sheet was 0°/PP/0°. The average plastic strain ratio of the sandwich sheet which was fabricated by the different direction combination (45°/PP/90°) in the upper/lower skin sheet was similar to the sandwich sheet which was fabricated by the same direction combination (0°/PP/0°), however, the planar anisotropy of the former was 3.2 times as low as the latter. Generally, the planar anisotropy of the sheet

with the rolling texture is relatively high, however, the average plastic strain ratio and the planar anisotropy decreased with increasing the heat treatment temperature and time since the increasing heat treatment time could induce the rotation of crystal orientation. Therefore, the sandwich sheet with both of high plastic strain ratio and low planar anisotropy could be fabricated by utilizing the directionality controls than traditional heat treatment controls.

5. CONCLUSIONS

(1) Through the change of shape parameters (*l*/d parameter) by the symmetric rolling in room temperature, the shear deformation could be obtained and then the typical texture components were proved by γ-fiber ND//<111> and rot-C_{ND} {001}<110>.
(2) The plastic strain ratio of AA/PP/AA sandwich sheets (1.58) was improved compared with 5182 aluminum skin sheets (1.50), but the planar anisotropy showed the similar value as -0.53. Therefore, the planar anisotropy of the sandwich sheet was highly dependent on that of the 5182 aluminum skin sheet.
(3) To improve the planar anisotropy, the new manufacturing procedure using directionality combinations of the upper and lower sheet was suggested. The planar anisotropy of the AA/PP/AA sandwich sheet manufactured by the new procedure showed 0.17 and improved 3.2 times than that of the 5182 aluminum sheet.

REFERENCES

Asbeck, H. O. and Mecking, H. (1978). Influence of friction and geometry of deformation on texture inhomogeneities during rolling of Cu single crystals as an example. *Mater. Sci. Eng.*, **34,** 111–119.

Baeck, S. M., Seok, H. K., Lee, J. C. and Oh, K. H. (2001). *Texture Analysis of Aluminum Plate Produced by ECAP*, 2nd LIMAT, **II,** 621–626.

Cho, S.-S., Han, B. K., Chang, H. and Kim, B. K. (2005). Effects of forming process on sealing performance of full-bead of MLS gasket: Finite element analysis approach. *Int. J. Automotive Technology* **6, 2,** 191–196.

Choi, C. H. and Lee, D. N. (1995). Shear texture formation in cold rolled aluminum and its recrystallization texture. *Proc. of the 16th Risø Inter. Symp. of Mater. Sci., Denmark*, 289–294.

Choi, C. H., Kwon, J. W., Oh, K. H. and Lee, D. N. (1997). Analysis of deformation texture inhomogeneity and stability condition of shear components in f.c.c. *Metals, Acta. Metall.*, **45, 12,** 5119–5128.

Hasegawa, K., Fujita, T., Araki, K., Mitao, S., Osawa, K., Niikura, M. and Ohori, K. (1998). Effect of intermediate annealing on the R-value of Al-Mg alloy sheet. *Mater. Sci. and Eng.*, **A257,** 204–214.

Holscher, M., Raabe, D. and Lucke, K. (1994). Relationship between rolling textures and shear textures in F.C.C. and B.C.C. metals. *Acta Metall. Mater.* **42, 3,** 879–886.

Hu, J., Ikeda, K. and Murakami, T. (1996). Effect of single roller driving cold-rolling on texture and formability of pure aluminum sheet. *J. Japan Inst. Metals* **60, 11,** 1130–1135.

Hutchinson, W. B. (1989). Recrystallization textures in iron resulting from nucleation at grain boundaries. *Acta Mater.* **37, 4,** 1047–1056.

Jeong, H. T., Hong, S. H. and Lee, D. N. (1999). Variation of plastic strain ratios of brass sheet with tensile strain. *Textures and Microstructures*, **32,** 355–367.

Jeong, H. T., Um, K. K., Lee, D. N. and Szpunar, J. A. (2000). Variation of shear texture with shear to effective strain ratio in rolled FCC metal sheet. *THERMEC 2000, Symp. on Textures in Mater. - Int. Conf. on Proc. and Manuf. of Adv. Ma.*, Las Vegas, NV, USA, Nov., 4–8.

Kamijo, T. and Fukutomi, H. (1995). Improvement of lankford value in Al-Mg alloys by the formation of (111) recrystallization texture. *Proc. of the 16th Risø Inter. Symp. of Mater. Sci.*, Ed. N. Hansen, D. Juul, Y. L. Kiu and B. Ralph, Denmark, 377–382.

Kamijo, T., Adachihara, H. and Fukutomi, H. (1993). Formation of a (001)[100] deformation structure in aluminum single crystals of an S-Orientation. *Acta Mater.* **41, 3,** 975–985.

Kamijo, T., Adachihara, H., Fukutomi, H. and Aernoudt, E. (1992). Development of cube texture in aluminum single crystals of a stable orientation. *Acta Mater.* **40, 4,** 693–698.

Kamijo, T., Matukawa, K. Y. and Noguchi, N. (1972). Rolling and annealing texture in the outer layer of rolled aluminum sheet. *J. of Jap. Inst. Metals.*, **36,** 669–673.

Kim, K. H. (1999). Textures and plastic strain ratios of asymmetrically rolled aluminum alloy sheets. Ph.D. Dissertation of Seoul National Univ., 136–150.

Kim, K. J. (2005). Texture evolution of AA5182 aluminum alloy rolled sheets after annealing. *J. of Mater. Sci. Letter*, to be Published.

Kim, K. J., Kim, D., Choi, S. H., Chung, K., Shin, K. S., Barlat, F., Oh, K. H. and Youn, J. R. (2003). Formability of AA5182/Polypropylene/AA5182 sandwich sheets. *J. of Mater. Proc. Tech.* **139, 1/3,** 1–7.

Lee, C. S. and Duggan, B. J. (1991). A simple theory for the development of inhomogeneous rolling textures. *Metall. Trans. A*, **22A,** 2637–2643.

Lee, C. S., Smallman, R. E. and Duggan, B. J. (1994). Effect of rolling geometry and surface friction on cube texture formation. *Mater. Sci. and Tech.*, **10,** 149–154.

Lee, D. N. (1985). Theoretical dependence of limiting drawing ratio on plastic strain ratio. *Proc. of the 7th Inter. Conf. on the Strength of Metals and Alloys,* Montreal, Canada, 971–976.

Lee, D. N. and Oh, K. H. (1985). Calculation of plastic strain ratio from the texture of cubic metal sheet. *J. of Mater. Sci.*, **20,** 3111–3118.

Lee, D. N., Kim, K. H., Choi, C. H. and Kang, H. G. (1997). Improvement in formability of aluminum alloy sheets for use of automobiles. *Proc. Inter. Conf. on Adv. Auto. Mater.*, Beijing China, 67–76.

Lequeu, P. and Jonas, J. J. (1988). Modeling of the plastic anisotropy of textured sheet. *Metall. Trans.*, **19A,** 105–120.

Major, B. (1992). Texture, microstructure and stored energy inhomogeneity in cold rolled commercial purity aluminum and copper. *Mater. Sci. Tech.*, **8,** 510–515.

Park, J. J. (1999). Predictions of texture and plastic anisotropy developed by mechanical deformation in aluminum sheet. *J. of Mater. Proc. Tech.*, **87,** 146–153.

Pithan, C., Hashimoto, T., Kawazoe, M., Nagahora, J. and Higashi, K. (2000). Microstructure and texture evolution in ECAE processed A5056. *Mater. Sci. Eng.*, **A280,** 62–68.

Reid, C. N. (1975). *Deformation Geometry for Materials Scientists.* Pergamon Press. 111–178.

Rhee, M. H., Ryu, Y. M., Kim, K. J., Shin, K. S., Kim, J. H. and Lee, K. N. (2000). Development of application technique of aluminum sandwich sheets for automotive hood. *FISITA 2000*, Seoul, Korea, June 12–15.

Saito, Y., Utsunomiya, H., Suzuki, H. and Sakai, T. (2000). Improvement in the R-value of aluminum strip by a continuous shear deformation process. *Scripta Mater.*, **42,** 1139–1144.

Sakai, T., Hamada, S. and Saito, Y. (2001). Improvement of the R-value in 5052 aluminum alloy sheets having through-thickness shear texture by 2-pass single-roll drive unidirectional shear rolling. *Scripta Mater.*, **44,** 2569–2573.

Sakai, T., Saito, Y. and Kato, K. (1987). Recrystallization and texture formation in high speed hot rolling of austenitic stainless steel. *Trans. ISIJ*, **27,** 520–525.

Sakai, T., Saito, Y., Hirano, K. and Kato, K. (1988). Deformation and recrystallization behavior of low carbon steel in high speed hot rolling. *Trans. ISIJ*, **28,** 1028–1035.

Sakai, T., Saito, Y., Matsuo, M. and Kawasaki, K. (1991). Inhomogeneous texture formation in high speed hot rolling of ferritic stainless steel. *ISIJ Inter.*, **31.** 86–94.

Shin, K. S., Kim, K. J., Choi, S. W. and Rhee, M. H. (1999). Mechanical properties of aluminum/polypropylene/aluminum sandwich sheets. *Metals and Mater.* **5, 6,** 613–618.

Truszkowski, W., Krol, J. and Major, B. (1980). Inhomogeneity of rollong texture in fcc metals. *Metall. Trans. A*, **11A,** 749–758.

Truszkowski, W., Krol, J. and Major, B. (1982). On penetration of shear texture into the rolled aluminum and copper. *Metall. Trans. A*, **13A,** 665–669.

Veenstra, E. W. (1993). Aluminum-plastic-aluminum sandwich sheet for maximum weight reduction in body panels. *SAE Paper* 930706, 1–10.

APPENDIX

$$\sigma_x = \frac{\bar{\sigma}_y}{\Delta\bar{\varepsilon}} \boldsymbol{QCQ}^{-1} \Delta\varepsilon_x \tag{A1}$$

where, $\boldsymbol{C} = \boldsymbol{C}(\Delta x)$, is denoted by matrix contained material coefficients

Material coefficients of Equation (A1), H, F, G and N are directly related to the plastic strain ratios, R_0, R_{45} and R_{90}. Hardening curve is assumed as $\bar{\sigma} = K\bar{\varepsilon}^n\dot{\bar{\varepsilon}}^m$. Therefore, Equation (A1) becomes,

$$\sigma_x = \frac{K(\bar{\varepsilon})^n\left(\frac{\Delta\bar{\varepsilon}}{\Delta t}\right)^m}{\Delta\bar{\varepsilon}} \boldsymbol{QCQ}^{-1} \Delta\varepsilon_x \tag{A2}$$

where, K, n and m are the strength coefficient, work hardening exponent and strain rate sensitivity, respectively. And $\boldsymbol{Q}$ and $\boldsymbol{Q}^{-1}$ are tensor transform matrix and its transpose. Note that Equation (A2) is nonlinear equation, therefore, iterations should be carried out. For one layer sheet, governing Equation (A1) is sufficient to solve the R-value. However, as the sandwich sheet is composed of three layers, as shown in Figure (A-I), the boundary conditions at the interface of three layers should be concerned. For uniaxial tension test, the force equilibrium at loading direction is,

$$F_{xx}^{tot} = F_{xx}^1 + F_{xx}^2 + F_{xx}^3 \tag{A3}$$

and force equilibrium equations at extra directions which have free traction are,

$$F_{yy}^{tot} = F_{yy}^1 + F_{yy}^2 + F_{yy}^3 = 0 \tag{A4a}$$

$$F_{xy}^{tot} = F_{xy}^1 + F_{xy}^2 + F_{xy}^3 = 0 \tag{A4b}$$

And each layer is assumed to deform as same quantities,

$$\Delta\varepsilon_{xx}^{tot} = \Delta\varepsilon_{xx}^1 = \Delta\varepsilon_{xx}^2 = \Delta\varepsilon_{xx}^3 \tag{A5a}$$

$$\Delta\varepsilon_{yy}^{tot} = \Delta\varepsilon_{yy}^1 = \Delta\varepsilon_{yy}^2 = \Delta\varepsilon_{yy}^3 \tag{A5b}$$

$$\Delta\varepsilon_{xy}^{tot} = \Delta\varepsilon_{xy}^{1} = \Delta\varepsilon_{xy}^{2} = \Delta\varepsilon_{xy}^{3} \quad \text{(A5c)}$$

Equation (A3)~Equation (A4) are exchanged by stress and thickness terms,

$$\sigma_x^{tot} = \frac{1}{t^{tot}}\sum_i \sigma_x^i t^i \quad \text{(A6)}$$

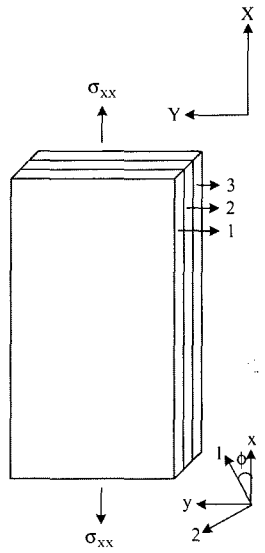

Figure A-I. Notation of uniaxial tension of AA/PP/AA sandwich sheet.

If Equation (A6) was investigated for *xx* direction components, Equation (A4) is described as following;

$$\sigma_{xx}^{tot} w t^{tt} = \sigma_{xx}^{1} w t^{1} + \sigma_{xx}^{2} w t^{2} + \sigma_{xx}^{3} w t^{3}$$

$$\sigma_{xx}^{tot} = \frac{1}{t^{tot}}(\sigma_{xx}^{1} t^{1} + \sigma_{xx}^{2} t^{2} + \sigma_{xx}^{3} t^{3})$$

$$\sigma_{xx}^{tot} = \frac{1}{t^{tot}}\sum_i \sigma_{xx}^i t^i$$

where, t and w are thickness and width, respectively. Equation (A1) was substituted to Equation (A6) with applying to the compatibility conditions at the interface of each layer, Equation (A6) becomes,

$$\sigma_x^{tot} = \sum_i \frac{t^i}{t^{tot}}\sigma_x^i = \left[\sum_i \frac{t^i}{t^{tot}}\left(\frac{\bar{\sigma}^i}{\Delta\bar{\varepsilon}^i}\right)\boldsymbol{Q}^i \cdot \boldsymbol{C}^i \cdot (\boldsymbol{Q}^{-1})^i\right] \cdot \Delta\varepsilon_x^{tot} \quad \text{(A7)}$$

In Equation (A7), bold characters represent vector, each vector component is as following;

$$\Delta\varepsilon_x^1 = \begin{bmatrix} \Delta\varepsilon_{xx}^1 \\ \Delta\varepsilon_{yy}^1 \\ \Delta\varepsilon_{xy}^1 \end{bmatrix}$$

When nonlinear equation of Equation (A7) is numerically solved by iteration, the strain controller values, $\Delta\varepsilon_{xx}^{tot}$ are given. Considering uniaxial tension test, force boundary conditions are prescribed as following;

$$\sigma_{yy}^{tot} = 0$$

$$\sigma_{xy}^{tot} = 0$$

And unknowns are,

σ_{xx}^{tot}

$\Delta\varepsilon_{yy}^{tot}$

$\Delta\varepsilon_{xy}^{tot}$

Therefore, this problem is a set of three equations and three unknowns.